

HEALTH AND MEDICINE

An ultraportable and versatile point-of-care DNA testing platform

Huan Xu¹, Anyue Xia², Dandan Wang³, Yiheng Zhang⁴, Shaoli Deng⁵, Weiping Lu⁵, Jie Luo⁶, Qiu Zhong⁵, Fengling Zhang⁵, Lin Zhou¹, Wenqing Zhang¹, Yang Wang¹, Cheng Yang¹, Kai Chang¹, Weiling Fu¹, Jinhui Cui^{3,*}, Mingzhe Gan^{3,7,*}, Dan Luo^{8,9,*}, Ming Chen^{1,10,11*}

Point-of-care testing (POCT) has broad applications in resource-limited settings. Here, a POCT platform termed POCKET (point-of-care kit for the entire test) is demonstrated that is ultraportable and versatile for analyzing multiple types of DNA in different fields in a sample-to-answer manner. The POCKET is less than 100 g and smaller than 25 cm in length. The kit consists of an integrated chip (i-chip) and a foldable box (f-box). The i-chip integrates the sample preparation with a previously unidentified, triple signal amplification. The f-box uses a smartphone as a heater, a signal detector, and a result readout. We detected different types of DNA from clinics to environment to food to agriculture. The detection is sensitive (<10³ copies/ml), specific (single-base differentiation), speedy (<2 hours), and stable (>10 weeks shelf life). This inexpensive, ultraportable POCKET platform may become a versatile sample-to-answer platform for clinical diagnostics, food safety, agricultural protection, and environmental monitoring.

Copyright © 2020
The Authors, some
rights reserved;
exclusive licensee
American Association
for the Advancement
of Science. No claim to
original U.S. Government
Works. Distributed
under a Creative
Commons Attribution
NonCommercial
License 4.0 (CC BY-NC).

INTRODUCTION

Laboratory-based detection methods such as polymerase chain reaction (PCR) are typically unavailable in resource-limited settings, where sophisticated infrastructures, reliable electricity supplies, and trained operators are lacking. Point-of-care testing (POCT), on the other hand, permits rapid on-site detections in these locations. Consequently, any form of molecular detection including DNA analyses requires POCT (1–2).

Over the last 5 years, POC DNA analysis research has progressed rapidly not only in clinical cares but also in agriculture, environmental protection, and food safety (3–6). Two keys to the success of practical applications are the portability and versatility of POCT. For the portability issue, one of the greatest challenges has been to ensure the portability throughout the entire process, from sample preparation to signal amplification to readouts without additional instruments. Many recent efforts have been dedicated to improving the portability of the signal amplification step (7–8). For example, paper-based DNA detection methods, such as lateral flow assays, offered the portability for DNA binding and fixing (onto thin strips of papers), but still requiring additional instruments such as a centrifuge for sample preparation and a thermal incubator or thermal cycler for

enzyme reactions. In addition, most instruments required an alternating current (AC) power supply. The needs for instrument in the sample preparation stage and/or AC power supplies have severely limited the portability of the entire POCT. Although various methods without using an AC power such as using exothermic chemical reactions or positive temperature coefficient heaters had been developed to achieve isothermal amplification (9–12), those methods still weighed from hundreds to thousands of grams, too heavy to be ultraportable.

Versatility is another great challenge for POCT. The ideal DNA POCT system needs not only to be able to process diverse types of samples (such as saliva, urine, and blood) but also to be able to detect the multiple forms of DNA targets including pathogen-specific DNA sequences, gene mutations, single-nucleotide polymorphisms (SNPs), and allele genes (13–14). So far, it is still difficult to detect pathogen-specific DNA directly from raw samples (e.g., saliva) in the fashion of “sample-in-result-out” (15). Considering the requirement of more accurate detection of other DNA target forms and compatibility with other biological samples (whole blood, etc.) containing more interferences, it is still quite challenging to develop a versatile POCT platform for the detection of multiple forms of DNA targets from diverse types of samples in the sample-to-answer manner.

In this study, we created a point-of-care kit for the entire test, the POCKET, as an ultraportable and versatile POCT platform. The POCKET platform was ultraportable: less than 100 g in weight and smaller than 25 cm in length, fitting into a quart-sized plastic bag or a regular-sized envelope (B5 size, 17 cm × 25 cm). The POCKET was ultraportable for the entire test process, from sample preparation to signal amplification to final readouts without any instrument. The POCKET was also versatile, detecting different types of DNA from a variety of sample sources, from clinics (blood, buccal, and urine) to food (milk) to environment (river water) and to agriculture (plant leaves).

The POCKET was made of only two components: an integrated chip (i-chip), for both sample preparation and signal amplification, and a foldable detection box (f-box), using a smartphone as a heater, an incubator, a detector, and a result reader. The i-chip was smaller than fingertip and was fabricated using three-dimensional (3D) printing

¹Department of Clinical Laboratory Medicine, Southwest Hospital, Third Military Medical University (Army Medical University), Chongqing 400038, China. ²First Affiliated Hospital with Nanjing Medical University (Jiangsu Province Hospital), Nanjing 210029, China. ³CAS Key Laboratory of Nano-Bio Interface, Suzhou Institute of Nano-Tech and Nano-Bionics, Chinese Academy of Sciences, Suzhou 215123, China. ⁴Central Laboratory, Shanghai Cancer Institute, Renji Hospital, School of Medicine, Shanghai Jiao Tong University, Shanghai 200127, China. ⁵Department of Clinical Laboratory Medicine, Institute of Surgery Research, Daping Hospital, Third Military Medical University (Army Medical University), Chongqing 400042, China. ⁶Department of Clinical Laboratory, The 954th Hospital of Chinese People's Liberation Army, Xizang 856000, China. ⁷School of Nano-Tech and Nano-Bionics, University of Science and Technology of China, Suzhou 215123, China. ⁸Department of Biological and Environmental Engineering, Cornell University, Ithaca, NY 14853, USA. ⁹Kavli Institute at Cornell for Nanoscience, Cornell University, Ithaca, NY 14853, USA. ¹⁰College of Pharmacy and Laboratory Medicine, Third Military Medical University (Army Medical University), Chongqing 400038, China. ¹¹State Key Laboratory of Trauma, Burn and Combined Injury, Third Military Medical University (Army Medical University), Chongqing 400038, China.

*Corresponding author. Email: chming1971@126.com (M.C.); dl79@cornell.edu (D.L.); mzgan2010@sinano.ac.cn (M.G.); cjh8305@163.com (J.C.).

and microfabrication. The f-box was foldable for size reduction. The entire POCKET platform fitted within a quart-sized plastic bag or a regular-sized envelope (Fig. 1A). Furthermore, a previously unidentified heat-generating approach was created using only a smartphone; combined with the f-box, a smartphone-based isothermal incubator was realized without any conventional heaters, incubators, and AC power supplies (Fig. 1B, right). For the signal amplification, we developed a previously unidentified triple amplification method that combined an isothermal recombinase polymerase (iRP) amplification along with a further Au-silver complexes for a total of triple amplifications (termed iRPAS) (Fig. 1B, left top). The final amplified signals were colorimetric and were detected by the smartphone using the f-box (Fig. 1C). Thus, we achieved ultraportable from sample preparation to signal amplification to final readouts without any instrument.

Besides the ultraportability, the POCKET platform was versatile, capable of analyses of multiple types of DNA from a broad range of sources. First, the i-chip had Lego-type connectors 3D printed, rendering the POCKET platform readily expandable for the parallel detections of multiple samples. Second, the entire POCKET platform was designed to be generally usable for a variety types of DNA using samples from different sources. In other words, the POCKET was designed and constructed independent of what types of DNA were used. We successfully detected various types of DNA from clinical blood and buccal samples including gene mutations (long or short fragment deletions), SNPs (single-base substitution or insertion), and allele genes. We also successfully detected pathogen-specific DNA sequences from urine samples (Fig. 1D). The sensitivity and specificity of the detections were verified with the conventional clinical methods currently performed in a centralized laboratory. In addition to real clinical samples, with the POCKET platform, we

successfully detected the following specific DNA: bacteria in milk, river water, and on plant leaves, further demonstrating the versatility of the POCKET platform in sample sources.

RESULTS

Design strategy of the POCKET platform

The POCKET platform consisted of two major components: an i-chip and an f-box. The i-chip, only 4 g in weight, integrated two units: a 3D-printed sample preparation unit and a microfluidic signal amplification unit (Fig. 2A). For the 3D-printed sample preparation unit, we incorporated three modules: a basket, a rotary valve, and a block module. We designed an extraction disc at the bottom of the basket module for binding DNA from a broad range of sources (Fig. 2A, dotted box). The basket was connected to a polytetrafluoroethylene (PTFE) for injecting the reagents into the basket by a syringe. To streamline the delivery of reagents and to avoid using expensive pipetting tools, we developed a tandem reagent tube to preload and deliver reagents automatically. Each reagent was separated by an air gap such that multiple reagents were preloaded in a PTFE tube (fig. S1). The block module contained a wash chamber, which was fit with the basket module for DNA purification, and a reaction chamber, which was fit with the rotary valve for target DNA amplification through recombinase polymerase amplification (RPA). The rotary valve was designed as a hollow cylinder with a pore near the bottom side of the module for the connection with microfluidic signal amplification unit. There was another pore on the reaction chamber of the block module connecting with the microfluidic signal amplification unit through a PTFE tube. The open and close states of the microfluidic amplification unit connection were controlled by rotating the rotary valve.

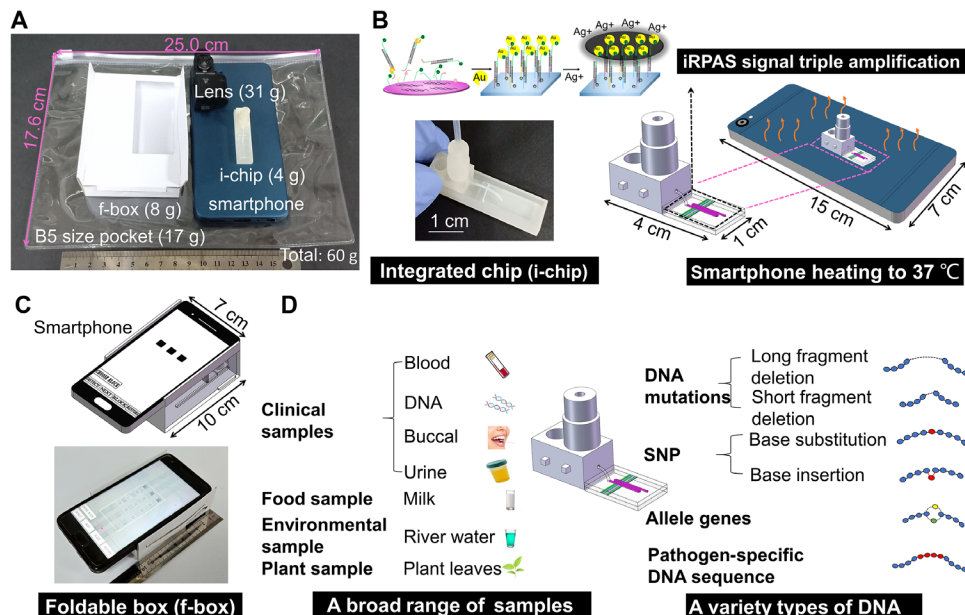


Fig. 1. POCKET platform was ultraportable and versatile. (A) The POCKET platform consisted of an i-chip and f-box, which was ultraportable (60 g) and stored in a B5-sized pocket. (B) During signal amplification, the i-chip was heated by a smartphone with no additional heating instrument (right). A visual signal was generated by iRPAS signal triple amplification (top). The i-chip was designed to be smaller than one fingertip (lower left). (C) Schematic and photograph of smartphone-based f-box. (D) The POCKET platform enabled the analyses of long and short fragment deletions, single-base substitution, single-base insertion, and allele genes, in addition to pathogen-specific DNA sequences from a broad range of sources including blood, extracted DNA, buccal, urine, milk, river water, or plant leaves. Photo credit (A, B, and C): Huan Xu, Army Medical University.

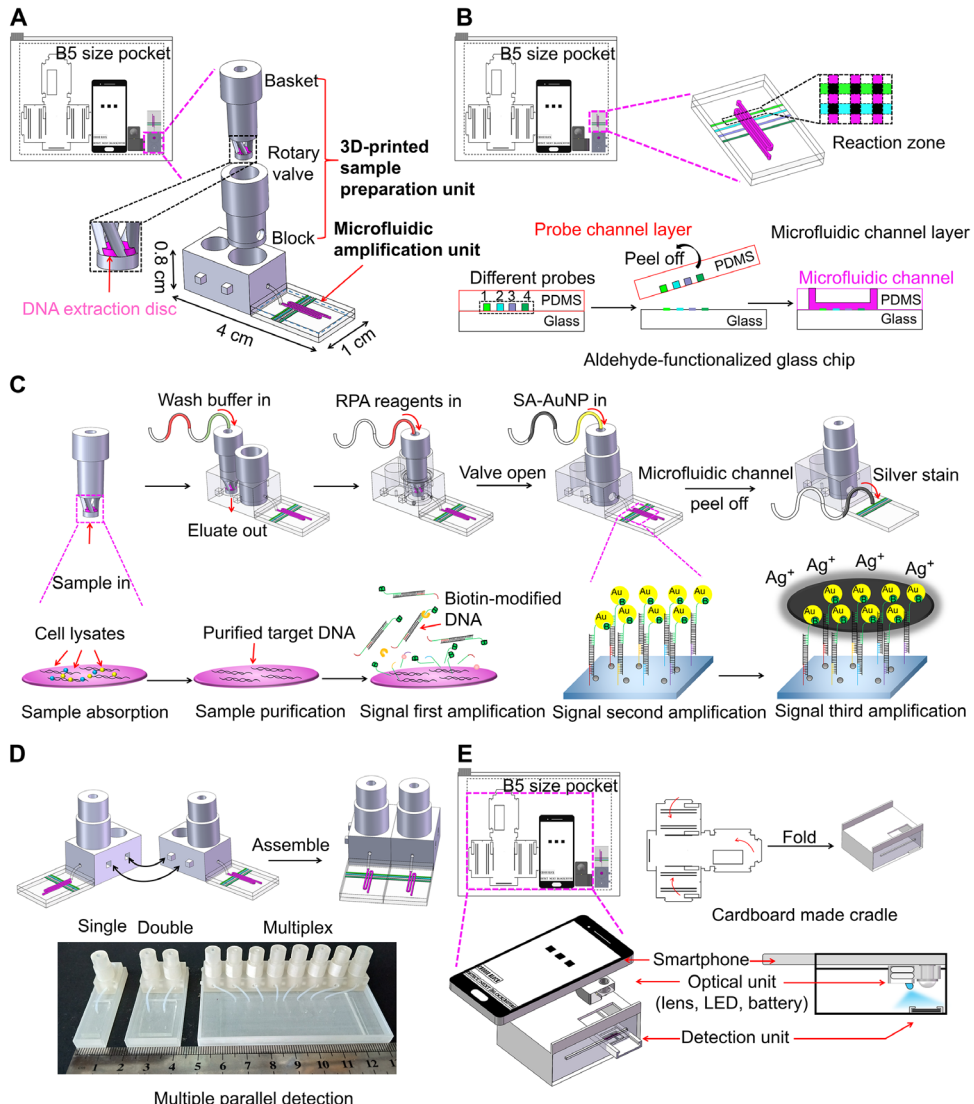


Fig. 2. Design and construction of POCKET platform. (A) Schematic of the i-chip (left). The i-chip consisted of a 3D-printed sample preparation unit and a microfluidic amplification unit. The sample preparation unit was designed to perform the entire process of POC DNA pretreatment using a basket module, a rotary valve, and a block module. The basket module had a DNA extraction disc at its bottom (dotted box). (B) Schematic of the microfluidic amplification unit. The microfluidic amplification unit consisted of a microfluidic channel layer and an aldehyde-functionalized glass chip. The probe channel layer (marked in red) was used to modify the capture probes on the aldehyde-functionalized chip. The microfluidic channel layer (marked in pink) was then assembled onto the chip to complete the amplification unit. The cross section of the probe fluidic and microfluidic channels constituted the reaction zone (dotted box). The numbers 1, 2, 3, and 4 on the probe channel layer indicated different probe channels with different colors. (C) Detection procedure of POCKET system. DNA was absorbed and extracted using the extraction disc at the bottom of the basket. Target DNA was purified using a wash buffer and amplified by RPA to obtain biotin-modified amplicons. The amplicons were bound to SA-AuNPs and captured by premodified capture probes to achieve a secondary signal amplification. The tertiary amplification was initiated by depositing silver ions onto the AuNPs. (D) The POCKET platform was scalable for parallel sample detections by i-chips assembly. (E) Schematic of the f-box, which was designed to display the results. This included a foldable cradle, a smartphone, an optical unit with a macro-lens, and a LED lamp. Photo credit (D): Huan Xu, Army Medical University.

The microfluidic amplification unit consisted of a microfluidic channel layer and an aldehyde-functionalized glass chip, designed for visual readouts via a smartphone (Fig. 2B). The glass chip was modified with multiple DNA capture probes, which were complementary to their targets. To fix capture probes on the glass chip, we first bound a polydimethylsiloxane (PDMS)-made probe channel layer that contained multiple channels onto the aldehyde-functionalized glass. Then, we infused each channel with one type of amino-functionalized capture probe. The probes were bond on the glass surface through aldimine condensation. Next, we peeled off the probe

channel layer and assembled the microfluidic channel layer on top of the glass chip to complete the amplification unit (Fig. 2B, bottom, and fig. S2). The surface density of the capture probe was critical for the function of sensing layer (16). We optimized the capture probe concentrations and found that 6 μ M was ideal to give a reliable result with approximately 10-fold signal increase (fig. S3A).

To amplify signals to such an extent that they could be visualized by naked eyes or a smartphone, we developed a previously unidentified iRPAS signal triple amplification method (Fig. 2C). Briefly, DNA was first amplified through RPA by tail-forward primers and biotinylated

reverse primers for 20 min, resulting in biotin-modified, tailed amplicons. The reaction was transferred to the channel of microfluidic unit, and the biotin-modified amplicons were captured by the previously mentioned capture probes. The second amplification was through the affinity binding of biotin with the streptavidin-conjugated gold nanoparticles (SA-AuNPs), and the hybridization time was optimized to 15 min (fig. S3B). The third amplification was completed through a silver ion catalytic cascade that resulted in more and more silver ions deposited on the AuNPs. After this iRPAS signal triple amplifications, the signal was visualized by the naked eyes or semiquantified by a smartphone. The entire operation procedure for user was simple including five steps, and the operation time was short, less than 80 min (fig. S4).

Notably, the entire i-chip was designed with a Lego-like mortise and tenon connections for simple assembly and to allow multiple sample analyses in parallel (Fig. 2D). Thus, the POCKET platform was readily scalable for multiple DNA analyses.

Most enzyme-based DNA detection methods such as PCR and loop-mediated isothermal amplification (LAMP) require a bulky thermal cycler or an incubator. Not surprisingly, current POC systems still require an additional heat supply, such as an incubator or an exothermic chemical package (11, 17, 18). Here, to make our POCKET ultraportable without any additional instrument, we took the advantage of the heat generated by a smartphone and deliberately used that heat for maintaining an isothermal incubation at 37°C, the optimized temperature for RPA. In more detail, we programmed a smartphone application (called “heat-up” application) whose algorithm called for intense central processing unit operations that resulted in a rapid temperature increase of the smartphone. By controlling both the number and timing of the algorithms running, we precisely controlled the temperature of the smartphone (fig. S5A). The heat transfer from the smartphone to the chip was almost instantaneously due to the extremely small nanoliter volume. To prevent heat dissipation in cold environments, we constructed a thermos packet with the aluminum foil to reduce heat loss in cold environments (4°C). We also incorporated a temperature display bar (30° to 40°C with 2°C interval) that reported internal temperature in real time. Two additional temperature indication discs were also included to record whether the temperature was too cold (<37°C) or too hot (>42°C) (fig. S5B). To prevent smartphone from the biohazard, we put the smartphone into a disposable plastic bag to insulate from clinical samples, while the smartphone can still heat the chip outside the bag. After the detection, the bag can be recycled or disposed. We compared the smartphone-heating effects with and without the disposable plastic bag, and found that the enclosing bag had little impact on the smartphone heating after 20-min smartphone heating (fig. S6).

For signal readouts, we designed an f-box that integrated a smartphone, a smartphone cradle, and an optical unit with a macro-lens and a light-emitting diode (LED) (Fig. 2E). The smartphone cradle was designed to be foldable and fabricated from light-weight cardboard (fig. S7). The manufacturing cost of the disposable part of our platform is less than \$4.1, and the reusable part is less than \$2.5 (table S1). In comparison to the commercial devices such as GeneXpert IV (\$17,000), our platform is very cost-effective.

Multiple types of DNA analyses

To develop the POCKET into a versatile platform, we tested different kinds of DNA including gene mutations (long and short fragment deletions), SNPs (single-base substitutions and insertions), allele genes,

and pathogen-specific DNA sequences. To verify the false-negative result caused by poor DNA preparation, we added an inherent gene (human hemoglobin gene, *hbh*) in blood samples as an internal control. We can now distinguish the negative result between poor DNA preparation and no target: If both the internal control and the target are negative, then it indicates the poor DNA preparation. If the internal control is positive but the target is negative, then it indicates no target. We showed the results of positive, negative, and the poor DNA preparation in fig. S8. For the detection of long fragment deletions, we tested a 19-kb deletion of the Southeast Asia (SEA) α -thalassemia gene. Note that RPA was typical only for the amplification of sequences smaller than 500 base pairs, not for long fragments (19). Nevertheless, with the POCKET system and the designed paired primers (fig. S9A), we detected significant differences between the mutant sample and the healthy control; the results were further validated by DNA sequencing (Fig. 3A).

For the detection of other gene mutations, SNPs, and allele genes, we used terminal mismatch primers using a special kind of nucleic acids, the locked nucleic acids (LNAs). LNA is nucleic acid chemically modified by the addition of a 20-O, 40-C methylene bridge. LNA showed an increased specificity in the previously reported SNP detection (20). In addition, the introduction of mismatches in the primer, especially in the terminal ends, notably inhibited polymerase extension and thus discriminated the wild type and mutant types (fig. S9B) (21). We chose the following diseases for the gene mutations and SNP tests by the POCKET system: (i) β -thalassemia, a worldwide hereditary anemia that contained different types of gene mutations [we detected the CD41 mutation (four-base deletion) (Fig. 3B), the CD17 mutation (single-base substitution) (Fig. 3C), and the CD71 mutation (single-base insertion) (Fig. 3D)], and (i) allele genes (human ALDH2 gene), which correlated strongly with susceptibility to alcohol intoxication. In each case (Fig. 3, E to G), we obtained strong signals in the mutant samples and little to no signal in control samples. The results were further validated by DNA sequencing (Fig. 3, A to G, bottom).

Moreover, for the detection of the pathogen-specific DNA sequences, patient urine samples were successfully tested and diagnosed for two common bacterial urinary tract infections, *Escherichia coli* and *Klebsiella pneumoniae* (*K. pn*), via paired primers against conserved sequence regions (Fig. 3, H and I).

To summarize, the POCKET system showed versatility in detection of all types of DNA with single-base specificity including but not limited to gene mutations. Also, the entire test essentially remained the same among different DNA types; the only major alteration was to design different primers (table S2).

DNA detection in other fields beyond clinical medicine

In clinical medicine, the POCKET platform was very successful for detections of α -thalassemia and β -thalassemia in blood samples, ALDH2 in buccal swabs, and pathogens in urine samples. To further expand the versatility of the POCKET system in other areas, we explored its utility in food safety, agricultural protection, and environmental monitoring (Fig. 3, J to L).

For food safety applications, we mimicked food contamination by spiking 10^4 copies of *E. coli* in 1 ml of sterile milk. The POCKET system successfully detected the contamination (Fig. 3J) without much alterations for the entire test. For environmental protection, we chose river water spiked with *E. coli* as our model. Again, even with a vast amount of environmental impurity such as sand and microorganisms,

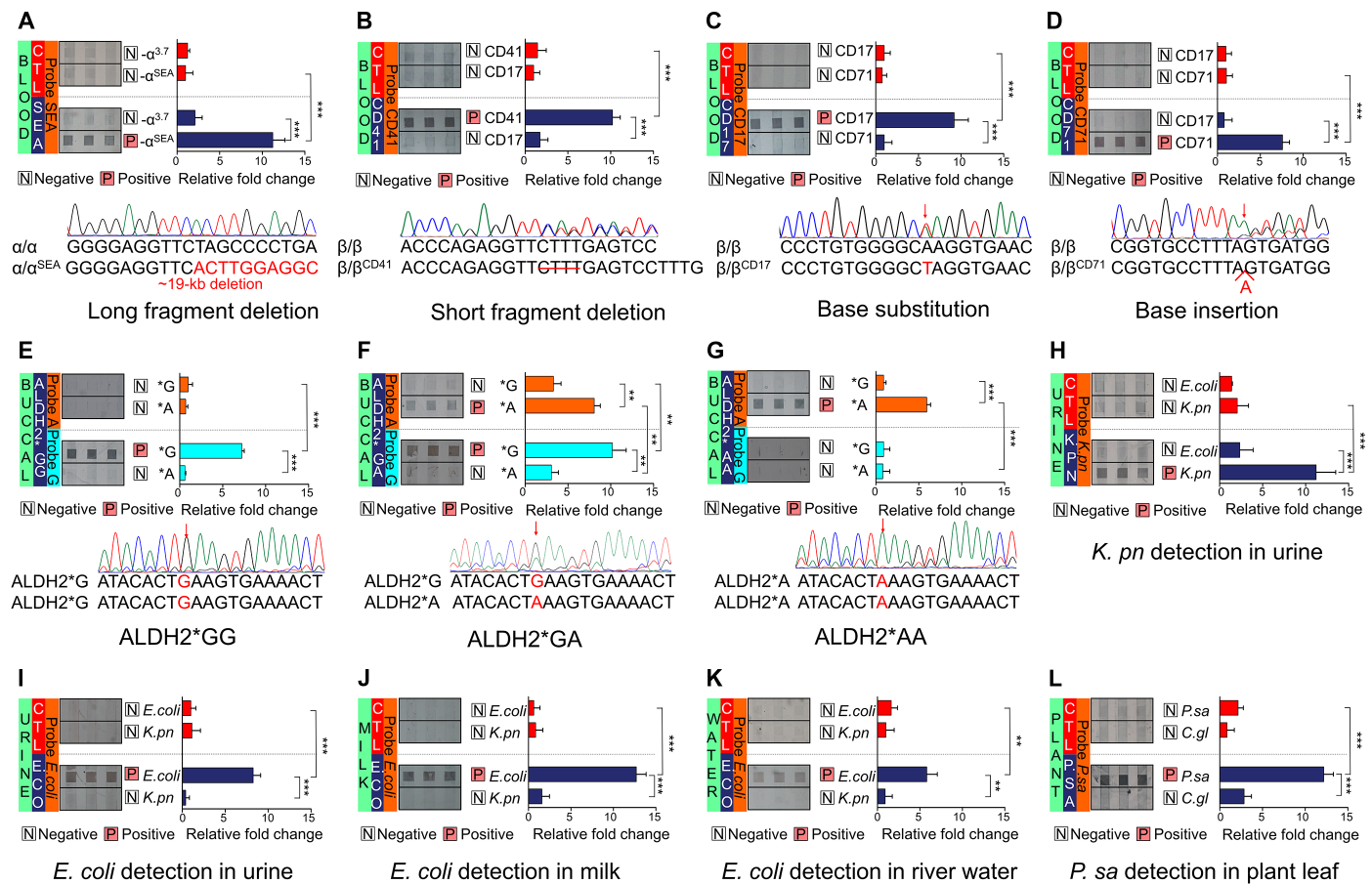


Fig. 3. DNA analysis using the POCKET platform. (A) Detection results from blood sample with SEA α -thalassemia mutation (~19-kb deletion), representing long fragment deletion. $-\alpha^{3.7}$ α -thalassemia mutation was used as negative control. (B) Detection results from blood sample with CD41 β -thalassemia mutation (TCTT deletion, marked with a red line), representing short fragment deletion. (C) Detection results from blood sample with CD17 β -thalassemia mutation (adenine substituted by thymine, marked in red), representing single-base substitution. (D) Detection results from blood sample with CD71 β -thalassemia mutation (adenine inserted, marked in red), representing single-base insertion. (E to G) Detection results from buccal swap samples with allele genes of ALDH2. Left (E), middle (F), and right (G) are homozygous wild-type (ALDH2*GG), heterozygote (ALDH2*GA), and homozygous mutant (ALDH2*AA), respectively. (H) Detection results from *K. pn*-infected patient urine sample. (I) Detection results from *E. coli*-infected patient urine sample. (J) Detection results from spiked *E. coli*-infected milk sample. (K) Detection results from spiked *E. coli*-infected river water sample. (L) Detection results from *P. sa*-infected kiwifruit leaves. *C. gl* was used as negative control. Each displayed signal was $200 \mu\text{m} \times 200 \mu\text{m}$ (A to L, top left), semiquantified by grayscale value (A to L, top right) and further validated by DNA sequencing (A to G, bottom). The green rectangle represents the sample type. Blue and red rectangles represent the mutant and healthy control (CTL) group. Orange and cyan rectangles represent probes used in POCKET detection. Data represent mean \pm SD (three repeats). *** $P < 0.001$, ** $P < 0.01$, Student's *t* test. N.S., not significant.

we successfully detected the 10^4 copies of spiked *E. coli* in 1 ml of the river water sample (Fig. 3K). For agriculture protection, it had been notoriously difficult for plant sample preparation in POC device due to the presence of strong inhibitory compounds such as lignin, polysaccharides, and phenolics in the sample (22). To more efficiently prepare plant samples, we 3D-printed a miniaturized grinding pestle and mortar (fig. S10). We successfully detected *Pseudomonas syringae* pv. *actinidiae* (*P. sa*), a common fruit tree pathogen, in kiwifruit leaves using our POCKET system (Fig. 3L).

These results confirmed that the POCKET platform was versatile in sample resources, not only in clinical applications but also in food safety, agricultural protection, and environmental monitoring.

Performance of the POCKET system in the field

The performance of the POCKET system, from temperature control to comparison of gold standard methods, was evaluated. For the

temperature control (e.g., in winter or in summer), we programmed and tested our heat-up application on a smartphone to reach the optimal 37°C in different environmental temperatures (4° , 15° , 25° , or 37°C). In each case, it took no longer than 20 min to reach and maintain 37°C (Fig. 4A). Strong signals were obtained under all tested temperatures (Fig. 4B). We also measured battery performance of the smartphone at each environmental temperature. At least four entire tests were completed without charging (battery 3400 mAh) (fig. S11A).

The performance parameters of POCKET were evaluated. For the limit of detection (LOD) of the system, we used a serial 10-fold dilution of plasmid DNA (from 1×10^{10} to 10 copies/ml) as standard samples. As expected, the detection signal decreased along a sigmoidal function as the logarithm of the target concentration decreased (Fig. 4C). The LOD, defined as “blank using distilled water plus three times standard deviation” (23), was calculated to be 113 copies/ml (Fig. 4D).

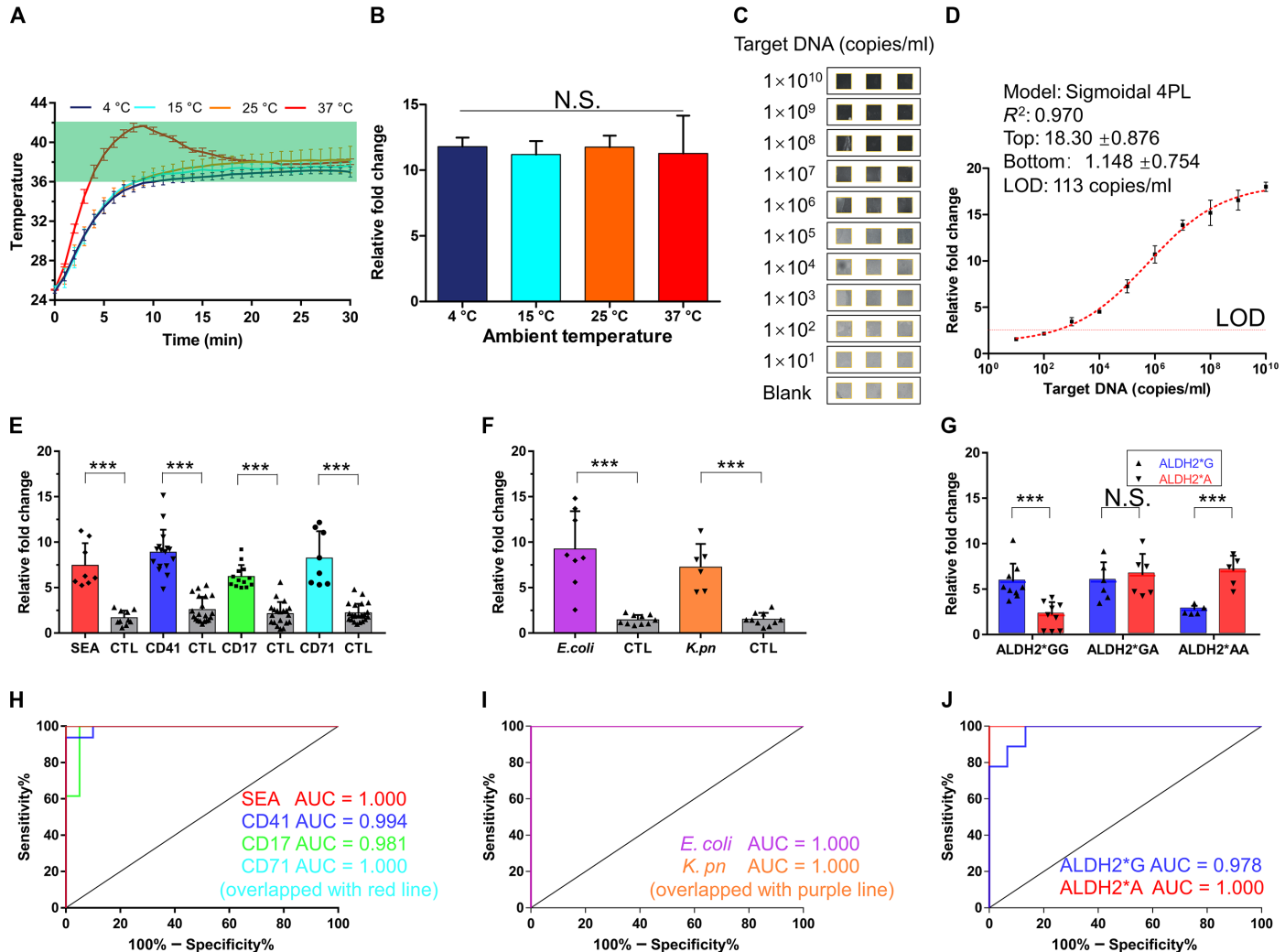


Fig. 4. Detection performance of the POCKET platform. (A) Temperature profiles using smartphone heating in 4°, 15°, 25°, and 37°C field conditions. Green bar indicates recommended reaction temperature range for RPA. (B) Detection performance of POCKET platform in 4°, 15°, 25°, and 37°C ambient temperature. N.S., not significant. One-way analysis of variance (ANOVA). (C) LOD of the platform was determined by 10-fold dilution of plasmid DNA and measuring their visual signals. All tests were performed in triplicate. (D) Calibration curve of the detection platform. Red dotted line indicates the LOD: 113 copies/ml. (E) SEA, CD41, CD17, and CD71 thalassemia mutations were measured from clinical peripheral venous blood samples and DNA samples purified from blood ($n = 118$, means of three repeats each). *** $P < 0.001$, Student's *t* test. (F) *E. coli* and *K. pn* were measured from patient urine samples ($n = 34$, mean of three repeats each). *** $P < 0.001$, Student's *t* test. (G) Homozygous wild-type (ALDH2*GG), heterozygote (ALDH2*GA), and homozygous mutant (ALDH2*AA) samples were measured from clinical buccal swabs ($n = 20$, means of three repeats each). *** $P < 0.001$, Student's *t* test. (H) ROC curves of SEA, CD41, CD17, and CD71 mutants were analyzed in mutant and healthy control (CTL) samples. The area under the curve (AUC) values were calculated as follows: SEA, 1.000; CD41, 0.994; CD17, 0.981; CD71, 1.000. (I) ROC curves of *E. coli* and *K. pn* of infected and CTL samples were compared. The AUC values were calculated as 1.000 (*E. coli*) and 1.000 (*K. pn*). (J) ROC curves for ALDH2*G and ALDH2*A were analyzed in three groups. The AUC values were calculated to be 0.978 (ALDH2*G) and 1.000 (ALDH2*A).

We also investigated the shelf life of i-chips without cold storage by keeping a batch of i-chips in a 25°C incubator up to 10 weeks. We then used them for detection once per week. No significant changes in results were observed after 10 weeks ($P < 0.05$), indicating that the i-chip was stable for at least 10 weeks without cold storage (fig. S11B).

For user friendliness, we compared the detection performance from a trained user group (previously already performed the POCKET at least three times) versus an untrained user group (the first time using the POCKET). No significant differences between the two groups were observed, suggesting that the POCKET system was very easy to perform and very user-friendly (fig. S11C). Furthermore, as a smartphone was the only nondisposable and expensive piece of in-

strument used in our system, we tested our POCKET performance using different brands of smartphones. The results showed no significant differences among any of three brands tested (fig. S11D).

The performance of the POCKET system was compared with conventional gold standard methods currently used in a centralized laboratory. Toward that end, we collected a total 172 samples including 63 peripheral venous blood samples, 55 DNA samples purified from participants' blood, 20 buccal swabs, and 34 urine samples. To show the robustness of our DNA testing using the POCKET platform in clinical samples, we tested the clinical samples with common abnormalities. We summarized the abnormal characteristics of the clinical samples including some strong interferences

(such as background cells, hemoglobin, and platelet) in table S3. In blood samples, the samples included a wide range of RPA interference concentrations (12 samples with abnormal red blood cell from 3.3×10^{12} to 6.9×10^{12} cells/liter, 46 samples with abnormal hemoglobin from 52 to 159 g/liter, 13 samples with abnormal platelet from 101×10^9 to 555×10^9 counts/liter). In urine samples, the samples also included a wide range of background cells (19 samples with abnormal red blood cells: 1 to 48,948 cells/ μ l, 24 samples with abnormal white blood cells: 1 to 47,577 cells/ μ l, 8 samples with abnormal epithelial cells: 1 to 295 cells/ μ l) (table S4). All samples were successfully analyzed using the POCKET system. They were also analyzed using standard methods including a thalassemia detection kit (a commercial clinical kit) for DNA and blood samples, DNA sequencing for buccal samples, and bacterial culture for urine samples (Fig. 4, E to G). The POCKET system showed successful detections. The total accuracy of our device for clinical samples is 97.1%, verified by laboratory standard methods: DNA sequencing for blood, buccal, and DNA samples, bacteria culture, and mass spectrometry for urine samples. (table S5). Further, receiver-operating characteristic (ROC) curves were plotted to determine the area under the curve (AUC) (Fig. 4, H to J). High AUC value over 0.9 was considered excellent accuracy (24). Each AUC in our POCKET detections was more than 0.950. Here, the POCKET platform achieved a higher detection accuracy, comparable to the gold standard methods performed in centralized laboratories.

We established the value of the maximum sensitivity as the cut-off value, which led to a decrease in specificity and positive predictive value (PPV). The POCKET platform still achieved 100% specificity and PPV for the detection of SEA, CD71, *E. coli*, *K. pn*, and ALDH2**A*. All other specificities were greater than 77.8%, and PPV was greater than 88.2% (Table 1). These results demonstrated that our POCKET system detected multiple targets with excellent performances.

DISCUSSION

Here, we established an ultraportable and versatile POCKET platform for DNA detection in nonlaboratory and resource-limited settings. To overcome the challenges from sample preparation to signal amplification to readouts in POCT workflow, we combined 3D printing, microfluidics, iRPAS signal amplification, and a smartphone. By 3D printing, miniaturized device prototypes can freely be fabricated with elaborate 3D structures, providing the high flexibilities in sample preparation and the fluid manipulation (25). Thus, a wide variety types of crude samples can be used in our POCKET platform. In many current POCT devices, including paper-based methods, clinical samples (e.g., blood) still rely on the laboratory-based pretreatments. It is difficult to perform direct, sample-to-answer detections in POC settings (26). We further adopted microfluidics and iRPAS signal amplification, enabling the sensitive, selective, and multiplexed testing on a chip. In addition to that, by producing the colorimetric signals, our POCKET eliminates the need of any optical filters, making the entire platform not only ultraportable and versatile but also more cost-effective, compared with fluorescence-based systems (17). We use a smartphone not only as a readout device for quantitative analyses but also as a heater, permitting the rapid and robust point-of-care DNA amplification even at the cold environment. Several heating methods exist in POCT using chemicals, peltier, and sunlight (9, 11, 17, 18). All of them require extra heating modules, resulting in more system weight and volume. Using a smartphone as a heater and readout device, we greatly reduce the weight and the volume of the whole platform, down to 60 g and the pocket size. As far as we know, the POCKET is the only platform that uses a smartphone itself as a heating supply. Because of our combinatory and integrated approach, the POCKET system was extremely light and small, rendering the POCKET system, to the best of our knowledge, to be one of the smallest and most portable POC DNA testing devices. Compared with other 3D-printed or microfluidic chips, our POCKET system was more versatile for a

Table 1. Detection performance of POCKET platform. Cutoff values were determined as the maximum sensitivity of the screening test. *N*, number of samples included for ROC analysis; 95% CI, 95% confidence interval; NPV, negative predictive value.

Target	Resource	Reference method	<i>N</i>	Cutoff value	AUC	95% CI	Sensitivity	Specificity	PPV	NPV
SEA	Peripheral venous blood	Reverse dot blot	18	4.053	1.000	1.000, 1.000	100.0%	100.0%	100.0%	100.0%
CD41	Purified DNA and blood	Reverse dot blot	36	4.720	0.994	0.977, 1.000	100.0%	90.0%	88.9%	100.0%
CD17	Purified DNA and blood	Reverse dot blot	33	4.544	0.981	0.940, 1.000	100.0%	95.0%	92.9%	100.0%
CD71	Purified DNA and blood	Reverse dot blot	31	5.070	1.000	1.000, 1.000	100.0%	100.0%	100.0%	100.0%
<i>E. coli</i>	Urine	Bacteria culture	18	2.416	1.000	1.000, 1.000	100.0%	100.0%	100.0%	100.0%
<i>K. pn</i>	Urine	Bacteria culture	16	3.700	1.000	1.000, 1.000	100.0%	100.0%	100.0%	100.0%
ALDH2*G	Buccal	DNA sequence	24	3.338	0.978	0.931, 1.000	100.0%	77.8%	88.2%	100.0%
ALDH2* <i>A</i>	Buccal	DNA sequence	16	3.700	1.000	1.000, 1.000	100.0%	100.0%	100.0%	100.0%

broader range of possible sample sources and achieved multiplex detections with reduced reagent costs (table S6) (6, 9, 11, 14, 17, 27–31).

Beside DNA testing, we are confident that our platform has the potential to detect more types of nucleic acids including but not limited to double-stranded DNA, single-stranded DNA, or RNA, considering that both DNA and RNA can be amplified through recombinase polymerase (14, 19, 32). Moreover, our POCKET system is extendable to nucleic acids detections in other fields beyond clinical medicine including but not limited to food safety, agriculture protection, and environmental monitoring. The sample sources can be from blood, urine, buccal swabs, milk, river water, leaves, etc.

With two billion smartphones already existing (2016) and even more by 2020 (covering more than 70% of the world population), smartphones are among the most convenient, user-friendly, and powerful interfaces for POC detection in resource-limited settings (33, 34). Smartphones are also most suitable for the signal processing and readouts in a POC setting. On the basis of smartphones' built-in wireless communication and geolocation capabilities, our POCKET platform makes it possible to real-time locate the distribution of the disease. Furthermore, the POCKET platform can serve as the Internet of Medical Things (IoMT) in DNA analysis to transmit on-site testing results to the centralized hospital or public health officials, providing spatiotemporal disease mapping for further investigation. In addition, end users including patients can receive fast feedbacks on disease control and prevention.

The POCT in this paper is our first version. In future improvements, we will expand the sample types to those that are known to be difficult to prepare, such as sputum and feces (35, 36). We will also further prevent cross-contamination from positive samples. The reagent loading method can also be better controlled using a power-free method (11, 37).

We envision that by prefabricating frequently emphasized targets on our chips, we will provide a series of comprehensive DNA detection panels for each separate application, from clinics to agriculture to environment to food and to drinking water. With further development, we firmly believe that the POCKET platform will become a widely used POCT device for a great number of real-world applications in various fields. We also hope that our POCKET system would become one of the gold standards for future POCT development.

MATERIALS AND METHODS

Fabrication of the i-chip

We designed the i-chip in SolidWorks software (SolidWorks, USA). Except for the microfluidic amplification unit, the i-chip was printed by a ProJet MJP 3600 3D printer using VisiJet M3 Crystal resin (3D Systems, USA). All freshly printed i-chips were heated in a 60°C oven to remove support wax and then washed in corn oil for 15 min. Last, printed i-chips were rinsed in water and dried in the nitrogen blow. In sample preparation unit, a small paper disc with the diameter of 2 mm was punched out from a large piece of DNA extraction paper (GE Lifescience, USA) using a Harris micro-punch. The paper disc was fitted in the basket module, which was then sealed in a plastic bag until required. The microfluidic amplification unit containing microfluidic channels with 200 μm width and 30 μm depth was fabricated using standard soft lithography as described previously (38). First, we made the chip mold on the glass slide by standard photolithography with the photoresist AZ4620 (AZ Electronic Materials, USA). PDMS prepolymer (Dow Corning, USA) was poured

onto the chip mold and cured at 90°C for 30 min. The cured PDMS was then peeled off the mold to yield the patterned channels. Then, the PDMS layer was treated following the previous report (fig. S2): first soaked in 20 ml of wash buffer (1% H₂O₂, 3 M HCl) for 10 min and then treated with 30 ml of 30% (3-aminopropyl)-trimethoxysilane (APTMS; Adamas, China) in water (39). After that, the PDMS layer was rinsed with water twice and then dried using the nitrogen blow. The PDMS layer was attached to the aldehyde-functionalized glass chip (Baio, China) for 1 hour and then vacuumed for 30 min. We designed two PDMS-made layers: the probe channel layer and the microfluidic channel layer. The probe channel layer was first bond to the glass chip. Then, 5 μM amino-functionalized DNA probes (Tsingke, China) in DNA spotting solution (CapitalBio, China) were then injected into each channel and incubated for 2 hours at room temperature to modify the probes on the surface of glass chip through aldimine condensation. The probe channel layer was then peeled off from the chip, which was then thoroughly washed with water and dried with the nitrogen flow. The freshly prepared microfluidic channel layer was then bound to the probe-modified glass chip to form microfluidic amplification unit. The amplification unit was fixed to the i-chip and connected to the preparation unit using a PTFE tube (inner diameter, 0.35 mm; Titan, China). The fabricated i-chip was stored at 4°C until use.

Construction of the f-box

We made the f-box with a foldable cradle, an optical unit with a white light LED (Supernatural Light, China) and a 60 \times macro-lens (Baisite, China), and a smartphone (Lenovo ZUK Z2, China). The cradle was designed by SolidWorks software and made by a white cardboard (0.4 mm thick). Then, the cardboard was cut to the designed pattern by a laser engraving machine (Shenhui, China). Afterward, we folded the cardboard into the cradle, as the eight folding steps of the assembling process illustrated in fig. S7, and then fixed the cradle by the designed slot. On the upside wall of the cradle, there was an open window for the insertion of the detection unit into the cradle. A 0.3-W white light LED powered by two 1.5-V button batteries was mounted above the detection unit for illumination. From the top window of the cradle, the macro-lens was plug in and aligned with the detection unit. The macro-lens was tightly fixed on the rear camera of the smartphone by a clamp.

Chip heating by smartphone

We controlled the chip heating by a heat-up application with functions of reading the internal temperature sensor and heating up the smartphone. The temperature was controlled by both the number and the time of the running algorithms. After the temperature reached 37°C, the i-chip was placed on the back of the smartphone for incubation. To avoid the heat loss and save the energy, the smartphone with the i-chip was placed in a thermos package with a temperature display bar (Jieyada, China). Then, the heating effects of the smartphone in the thermos package were tested in the incubator (Bluepard, China) at 4°, 15°, 25°, and 37°C. When testing the performance of smartphone heating in the cold environment (4°C), the smartphone with the i-chip was put in the thermos package and sealed by clips before placing in the incubator. The temperature of i-chip was real-time monitored by an external temperature recorder (Elitech, China).

Sample collection

The study was approved by the ethics committees of Daping Hospital and Southwest Hospital, Chongqing, China. Purified DNA samples,

buccal samples, and urine samples were collected from 55, 20, and 34 participants, respectively, from Daping Hospital, Chongqing, China. Peripheral venous blood samples from 63 participants were collected from Southwest Hospital, Chongqing, China. Spiked milk samples were mimicked by mixing 1 ml of sterile milk with *E. coli* [10^4 colony-forming units (CFU)/ml]. Spiked river water samples were prepared by mixing 1 ml of natural river water with 10^4 CFU/ml *E. coli*. *P. sa*-infected leaves and *Colletotrichum gloeosporioide* (*C. gl*)-infected leaves were obtained from X. Sun in Sichuan Agricultural University, Chengdu, China.

DNA sample preparation

We dipped the basket module into the sample liquid. About 2 μ l of sample was absorbed by the extraction paper disc at the bottom. We prepared leaf samples by the extra crushing as following steps. Five milligrams of leaves with 100 μ l of lysis buffer (Tiangen, China) was added to the 3D-printed mortar and grinded by the 3D-printed pestle for 5 min, and then 100 μ l of neutralizing buffer (Tiangen, China) was added and mixed thoroughly. The extraction paper disc with sample liquid was dried at room temperature for 10 min. Thereafter, the basket module was inserted into the wash chamber (inner diameter, 5.0 mm; height, 6.5 mm) of the sample preparation unit and washed with 200 μ l of purification reagent (GE Lifescience, USA) for 5 min and 200 μ l of TE buffer (10 mM tris-HCl and 0.1 mM EDTA, pH 8.0) for 5 min. Once washed, the basket module with purified sample DNA on the paper disc was pulled out from the wash chamber and dried at room temperature for 15 min.

RPA amplification

We performed the RPA amplification following the manufacturer's instructions (TwistDx, UK). For each reaction, 25 μ l of TwistDx 2 \times reaction buffer was mixed with 5 μ l of 10 \times basic E-mix, 3.6 μ l of 25 mM deoxynucleotide triphosphate, 6.6 μ l of nuclease-free water, and 2.5 μ l of core mix. Next, 4.8 μ l of primer mix, containing biotinylated reverse primer and tailed forward primer, was added to the RPA reaction reagent. Premixed RPA reaction reagent (47.5 μ l) and 2.5 μ l of magnesium acetate were successively infused into a PTFE tube (1.0 mm in inner diameter and 65 cm in length, Titan, China). Each reagent was separated by an air gap (over 5 cm in length) to form an isolated tandem reagent tube and stored at 4°C until required. At the start of amplification, the reagents in the isolated tandem reagent tube were injected into the reaction chamber (6.9 mm in inner diameter and 6.5 mm in depth) in the sample preparation unit by pushing air with a 1-ml syringe connecting to the tandem tube. The reaction was kept at 37°C for 20 min by the smartphone running with the heat-up application. All primers, amino-functionalized DNA probes, and LNA-modified probes (Zhanshan, China) were described in table S2. Plasmid (Tsingke, China) was described in fig. S12.

AuNP-silver amplification

After RPA amplification, we injected 50 μ l of hybridization buffer (5 \times Denhardt's solution, 3 \times saline sodium citrate, and 0.1% bovine serum albumin) containing 1% streptavidin-conjugated AuNPs (Nanoprobe, USA) into the reaction chamber to mix with the reacted RPA solution. Then, we opened rotary valve and injected the mixed solution into the microfluidic amplification unit through the connecting PTFE tube by pushing air with a 1-ml syringe. After that, the chip was incubated for 15 min by heating with the smart-

phone. The PDMS layer was then peeled off from the amplification unit, washed with water, and then stained with 20 μ l of silver enhance buffer (Sigma, USA) for 7 min. Last, after iRPAS signal triple amplification, the microfluidic amplification unit was imaged with a smartphone installed with the POCKET software application for signal readout.

POCKET software

The smartphone application "POCKET version 1.0" was designed to image capture and image process the input of basic sample information including sample barcode, location, and the upload of results to the cloud database. Briefly, the image was captured and converted to the 8-bit grayscale format and calculated its grayscale value (black as 0 and white as 255) within the regions of interest for the sample, reference, and background (fig. S13). First, the mean grayscale value of sample and reference were obtained by subtracting the background value. Next, the relative fold change was obtained by dividing the mean grayscale value of the sample with the reference. Last, the relative fold changes of samples were recorded and compared with the threshold to determine the positive or negative result. Here, the threshold was designated as the cutoff value for each target.

Detection verification

All purified DNA samples and peripheral venous blood samples were initially diagnosed using a thalassemia diagnostic kit (Hybribio, China) by reverse dot blot method and further verified by DNA sequencing (Invitrogen, China). For the verification of allele genes, the ALDH2 gene from buccal swabs was detected by DNA sequencing (Invitrogen, China). Bacteria in urine samples were cultured on the blood agar medium plate (Pangtong, China) and then diagnosed by the matrix-assisted laser desorption ionization-time of flight mass spectrometry (bioMérieux, France).

Data analysis and statistics

Statistical analysis was performed using GraphPad Prism 7.0 software (GraphPad Software, USA) and SPSS version 19.0 software (SPSS, USA). The data were normalized and expressed as mean \pm SD. Independent sample two-tailed Student's *t* tests were performed for comparisons between groups. Multiple-group statistical analyses were performed by one-way analysis of variance (ANOVA), with the least significant difference used for post hoc testing. *P* values <0.05 were regarded as statistically significant. Detection performance of the POCKET platform was calculated using area under ROC curves. As a screening test, cutoff values were selected on the basis of minimized false negatives, defined as the maximum sensitivity, taken at all points on the ROC curve.

SUPPLEMENTARY MATERIALS

Supplementary material for this article is available at <http://advances.sciencemag.org/cgi/content/full/6/17/eaaz7445/DC1>

[View/request a protocol for this paper from Bio-protocol.](#)

REFERENCES AND NOTES

1. P. K. Drain, E. P. Hyle, F. Noubari, K. A. Freedberg, D. Wilson, W. R. Bishai, W. Rodriguez, I. V. Bassett, Diagnostic point-of-care tests in resource-limited settings. *Lancet Infect. Dis.* **14**, 239–249 (2014).
2. P. Yager, G. J. Domingo, J. Gerdes, Point-of-care diagnostics for global health. *Annu. Rev. Biomed. Eng.* **10**, 107–144 (2008).
3. X. M. Sun, J. J. Wan, K. Qian, Designed microdevices for in vitro diagnostics. *Small Methods* **1**, 1700196 (2017).

4. H. Y. Lau, J. R. Botella, Advanced DNA-based point-of-care diagnostic methods for plant diseases detection. *Front. Plant Sci.* **8**, 2016 (2017).
5. M. Y. C. Wu, M. Y. Hsu, S. J. Chen, D. K. Hwang, T. H. Yen, C. M. Cheng, Point-of-care detection devices for food safety monitoring: Proactive disease prevention. *Trends Biotechnol.* **35**, 288–300 (2017).
6. N. R. Y. Ho, G. S. Lim, N. R. Sundah, D. N. Lim, T. P. Loh, H. L. Shao, Visual and modular detection of pathogen nucleic acids with enzyme-DNA molecular complexes. *Nat. Commun.* **9**, 3238 (2018).
7. M. Z. Yang, Y. Liu, X. Y. Jiang, Barcoded point-of-care bioassays. *Chem. Soc. Rev.* **48**, 850–884 (2019).
8. H. Xu, M. Gao, X. Tang, W. Zhang, D. Luo, M. Chen, Micro/nano technology for next-generation diagnostics. *Small Methods* **2019**, 1900506 (2019).
9. R. Snodgrass, A. Gardner, A. Semeere, V. L. Kopparthy, J. Duru, T. Maurer, J. Martin, E. Cesarmann, D. Erickson, A portable device for nucleic acid quantification powered by sunlight, a flame or electricity. *Nat. Biomed. Eng.* **2**, 657–665 (2018).
10. Y. Xu, Y. H. Liu, Y. Wu, X. H. Xia, Y. Q. Liao, Q. G. Li, Fluorescent probe-based lateral flow assay for multiplex nucleic acid detection. *Anal. Chem.* **86**, 5611–5614 (2014).
11. E. C. Yeh, C. C. Fu, L. Hu, R. Thakur, J. Feng, L. P. Lee, Self-powered integrated microfluidic point-of-care low-cost enabling (SIMPLE) chip. *Sci. Adv.* **3**, e1501645 (2017).
12. W. H. Zhou, L. Hu, L. M. Ying, Z. Zhao, P. K. Chu, X.-F. Yu, A CRISPR-Cas9-triggered strand displacement amplification method for ultrasensitive DNA detection. *Nat. Commun.* **9**, 5012 (2018).
13. C. E. Jin, B. Koo, E. Y. Lee, J. Y. Kim, S. H. Kim, Y. Shin, Simple and label-free pathogen enrichment via homobifunctional imidoesters using a microfluidic (SLIM) system for ultrasensitive pathogen detection in various clinical specimens. *Biosens. Bioelectron.* **111**, 66–73 (2018).
14. J. S. Gootenberg, O. O. Abudayyeh, M. J. Kellner, J. Joung, J. J. Collins, F. Zhang, Multiplexed and portable nucleic acid detection platform with Cas13, Cas12a, and Csm6. *Science* **360**, 439–444 (2018).
15. M. Zarei, Infectious pathogens meet point-of-care diagnostics. *Biosens. Bioelectron.* **106**, 193–203 (2018).
16. K. Chang, Y. Pi, W. P. Lu, F. Wang, F. Pan, F. K. Li, S. R. Jia, J. F. Shi, S. L. Deng, M. Chen, Label-free and high-sensitive detection of human breast cancer cells by aptamer-based leaky surface acoustic wave biosensor array. *Biosens. Bioelectron.* **60**, 318–324 (2014).
17. W. L. Chen, H. J. Yu, F. Sun, A. Ornob, R. Brisbin, A. Ganguli, V. Vemuri, P. Strzebonski, G. Z. Cui, K. J. Allen, S. A. Desai, W. R. Lin, D. M. Nash, D. L. Hirschberg, I. Brooks, R. Bashir, B. T. Cunningham, Mobile platform for multiplexed detection and differentiation of disease-specific nucleic acid sequences, using microfluidic loop-mediated isothermal amplification and smartphone detection. *Anal. Chem.* **89**, 11219–11226 (2017).
18. M. S. Draz, K. M. Kochehbyok, A. Vasari, D. Battalapalli, A. Seeram, M. K. Kanakasabapathy, S. Kallakuri, A. Tsibris, D. R. Kuritzkes, H. Shafiee, DNA engineered micromotors powered by metal nanoparticles for motion based cellphone diagnostics. *Nat. Commun.* **9**, 4282 (2018).
19. I. M. Lobato, C. K. O'Sullivan, Recombinase polymerase amplification: Basics, applications and recent advances. *Trac-Trends Anal. Chem.* **98**, 19–35 (2018).
20. K. N. Ballantyne, R. A. H. van Oorschot, R. J. Mitchell, Locked nucleic acids in PCR primers increase sensitivity and performance. *Genomics* **91**, 301–305 (2008).
21. Y. Shin, R. A. Soo, J. Yoon, A. P. Perera, Y. J. Yoon, M. K. Park, Rapid and label-free amplification and detection assay for genotyping of cancer biomarker. *Biosens. Bioelectron.* **68**, 107–114 (2015).
22. Y. P. Zou, M. G. Mason, Y. L. Wang, E. Wee, C. Turni, P. J. Blackall, M. Trau, J. R. Botella, Nucleic acid purification from plants, animals and microbes in under 30 seconds. *PLOS Biol.* **15**, e2003916 (2017).
23. L. Zhou, Y. Wang, C. Yang, H. Xu, J. Luo, W. Zhang, X. Tang, S. Yang, W. Fu, K. Chang, M. Chen, A label-free electrochemical biosensor for microRNAs detection based on DNA nanomaterial by coupling with Y-shaped DNA structure and non-linear hybridization chain reaction. *Biosens. Bioelectron.* **126**, 657–663 (2019).
24. J. N. Mandrekar, Receiver operating characteristic curve in diagnostic test assessment. *J. Thorac. Oncol.* **5**, 1315–1316 (2010).
25. H. N. Chan, M. J. A. Tan, H. K. Wu, Point-of-care testing: Applications of 3D printing. *Lab Chip* **17**, 2713–2739 (2017).
26. N. Kaur, B. J. Toley, Paper-based nucleic acid amplification tests for point-of-care diagnostics. *Analyst* **143**, 2213–2234 (2018).
27. K. Kadimisetty, J. Z. Song, A. M. Doto, Y. Hwang, J. Peng, M. G. Mauk, F. D. Bushman, R. Gross, J. N. Jarvis, C. C. Liu, Fully 3D printed integrated reactor array for point-of-care molecular diagnostics. *Biosens. Bioelectron.* **109**, 156–163 (2018).
28. J. H. Hui, Y. Gu, Y. S. Zhu, Y. J. Chen, S. J. Guo, S. C. Tao, Y. Zhang, P. Liu, Multiplex sample-to-answer detection of bacteria using a pipette-actuated capillary array comb with integrated DNA extraction, isothermal amplification, and smartphone detection. *Lab Chip* **18**, 2854–2864 (2018).
29. B. S. Ferguson, S. F. Buchsbaum, T. T. Wu, K. Hsieh, Y. Xiao, R. Sun, H. T. Soh, Genetic analysis of H1N1 influenza virus from throat swab samples in a microfluidic system for point-of-care diagnostics. *J. Am. Chem. Soc.* **133**, 9129–9135 (2011).
30. J. E. Kong, Q. Wei, D. Tseng, J. Zhang, E. Pan, M. Lewinski, O. B. Garner, A. Ozcan, D. DiCarlo, Highly stable and sensitive nucleic acid amplification and cell-phone-based readout. *ACS Nano* **11**, 2934–2943 (2017).
31. V. K. Rajendran, P. Bakthavathsalam, P. L. Bergquist, A. Sunna, A portable nucleic acid detection system using natural convection combined with a smartphone. *Biosens. Bioelectron.* **134**, 68–75 (2019).
32. S. M. Leong, K. M. Tan, H. W. Chua, M. C. Huang, W. C. Cheong, M. H. Li, S. Tucker, E. S. Koay, Paper-based microRNA expression profiling from plasma and circulating tumor cells. *Clin. Chem.* **63**, 731–741 (2017).
33. C. S. Wood, M. R. Thomas, J. Budd, T. P. Mashamba-Thompson, K. Herbst, D. Pillay, R. W. Peeling, A. M. Johnson, R. A. McKendry, M. M. Stevens, Taking connected mobile-health diagnostics of infectious diseases to the field. *Nature* **566**, 467–474 (2019).
34. Y. T. Zhao, M. M. Yang, Q. Q. Fu, H. Ouyang, W. Wen, Y. Song, C. Z. Zhu, Y. H. Lin, D. Du, A nanzyme- and ambient light-based smartphone platform for simultaneous detection of dual biomarkers from exposure to organophosphorus pesticides. *Anal. Chem.* **90**, 7391–7398 (2018).
35. M. Varona, X. Ding, K. D. Clark, J. L. Anderson, Solid-phase microextraction of DNA from mycobacteria in artificial sputum samples to enable visual detection using isothermal amplification. *Anal. Chem.* **90**, 6922–6928 (2018).
36. B. Y. Ng, E. J. Wee, N. P. West, M. Trau, Rapid DNA detection of *Mycobacterium tuberculosis*-towards single cell sensitivity in point-of-care diagnosis. *Sci. Rep.* **5**, 15027 (2015).
37. J. Deng, X. Jiang, Advances in reagents storage and release in self-contained point-of-care devices. *Adv. Mater. Technol.* **4**, 1800625 (2019).
38. Y. F. Tang, M. Z. Gan, Y. F. Xie, X. D. Li, L. W. Chen, Fast screening of bacterial suspension culture conditions on chips. *Lab Chip* **14**, 1162–1167 (2014).
39. X. Jiang, N. Shao, W. Jing, S. Tao, S. Liu, G. Sui, Microfluidic chip integrating high throughput continuous-flow PCR and DNA hybridization for bacteria analysis. *Talanta* **122**, 246–250 (2014).

Acknowledgments: We thank W. Jiang, H. Huang, T. Sun, and L. Liao from the Department of Clinical Laboratory, Daping Hospital, Chongqing, China. We are also grateful to X. Sun in Sichuan Agricultural University, Chengdu, China for the assistance with plant samples.

Funding: This work was supported by the National Natural Science Foundation of China (grants 81430053, 81430054, 81972027, 31400087, and 21778071), Chinese People's Liberation Army scientific research major projects (grant no. AWS14C003-2), Military Scientific Research Project of Army Medical University (2018XY04), and the Suzhou Institute of Nano-Tech and Nano-Bionics (Y5AA511001). M.G. acknowledges support from the Youth Innovation Promotion Association CAS (2015257). **Author contributions:** H.X., J.C., M.G., D.L., and M.C. designed the research. Y.Z. printed the 3D units. H.X., A.X., L.Z., F.Z., W.Z., Y.W., C.Y., and K.C. collected the samples. H.X., A.X., and D.W. performed the experiments. W.L., S.D., J.L., Q.Z., and W.F. analyzed the data. H.X., J.C., M.G., D.L., and M.C. wrote the manuscript. All authors reviewed the manuscript. **Competing interests:** H.X., J.C., M.G., and M.C. are listed as co-inventors on the pending Chinese patent application 201911218636.2, filed by Suzhou Institute of Nano-Tech and Nano-Bionics relating to this work at 3 December 2019. The authors declare no other competing interests. **Data and materials availability:** All data needed to evaluate the conclusions in the paper are present in the paper and/or the Supplementary Materials. Additional data related to this paper may be requested from the authors.

Submitted 5 October 2019

Accepted 6 February 2020

Published 22 April 2020

10.1126/sciadv.aaz7445

Citation: H. Xu, A. Xia, D. Wang, Y. Zhang, S. Deng, W. Lu, J. Luo, Q. Zhong, F. Zhang, L. Zhou, W. Zhang, Y. Wang, C. Yang, K. Chang, W. Fu, J. Cui, M. Gan, D. Luo, M. Chen, An ultraportable and versatile point-of-care DNA testing platform. *Sci. Adv.* **6**, eaaz7445 (2020).

Science Advances

An ultraportable and versatile point-of-care DNA testing platform

Huan Xu, Anyue Xia, Dandan Wang, Yiheng Zhang, Shaoli Deng, Weiping Lu, Jie Luo, Qiu Zhong, Fengling Zhang, Lin Zhou, Wenqing Zhang, Yang Wang, Cheng Yang, Kai Chang, Weiling Fu, Jinhui Cui, Mingzhe Gan, Dan Luo and Ming Chen

Sci Adv **6** (17), eaaz7445.
DOI: 10.1126/sciadv.aaz7445

ARTICLE TOOLS

<http://advances.sciencemag.org/content/6/17/eaaz7445>

SUPPLEMENTARY MATERIALS

<http://advances.sciencemag.org/content/suppl/2020/04/20/6.17.eaaz7445.DC1>

REFERENCES

This article cites 39 articles, 3 of which you can access for free
<http://advances.sciencemag.org/content/6/17/eaaz7445#BIBL>

PERMISSIONS

<http://www.sciencemag.org/help/reprints-and-permissions>

Use of this article is subject to the [Terms of Service](#)

Science Advances (ISSN 2375-2548) is published by the American Association for the Advancement of Science, 1200 New York Avenue NW, Washington, DC 20005. The title *Science Advances* is a registered trademark of AAAS.

Copyright © 2020 The Authors, some rights reserved; exclusive licensee American Association for the Advancement of Science. No claim to original U.S. Government Works. Distributed under a Creative Commons Attribution NonCommercial License 4.0 (CC BY-NC).